Earth and Planetary Science

https://journals.nasspublishing.com/index.php/eps

ARTICLE

Water Mass Vertical Mixing in The Sulawesi Sea and Makassar Strait During the Second Transition Monsoon

Shofia Karima [1,2*], ***Nining Sari Ningsih*** [3], ***Anastasia Rita Tisiana*** [4], ***Gandhi Napitupulu*** [3]

[1] *Master's Program in Earth Sciences, Faculty of Earth Sciences and Technology, Bandung Institute of Technology, Bandung 40132, Indonesia*

[2] *Research Center for Geological Disaster, National Research and Innovation Agency, Bandung 40293, Indonesia*

[3] *Environmental and Applied Oceanography Research Group, Faculty of Earth Science and Technology, Bandung Institute of Technology, Bandung 40132, Indonesia*

[4] *Agency for Marine and Fisheries Research and Human Resources, Ministry of Marine Affairs and Fisheries, Jakarta 14430, Indonesia*

ABSTRACT

The transformation of water masses along the Indonesian Throughflow (ITF) pathway is evident from the disappearance of Western North Pacific Water (WNPW) south of the Makassar Strait, despite its prior presence in the Sulawesi Sea. One of the primary mechanisms driving this transformation is vertical mixing. This study investigates the characteristics of vertical mixing along the Sulawesi Sea–Makassar Strait route during the second transition season (September–November), using vertical diffusivity (K_z) as a key indicator. The temperature, density, and current velocity data were obtained from the Transport, Internal Waves, and Mixing in the Indonesian Throughflow Regions (TIMIT) cruise in October 2015. The results show spatial variability of vertical mixing both horizontally and vertically. Horizontally, the strongest vertical mixing was observed in the Makassar Strait (K_z = 8.5 × 10^{-3} m^2/s and R_i = 2.0–2.2), consistent with values reported for the first transition season but exceeding those typical of the southeast monsoon. Vertically, mixing was most intense in the deep layer (K_z = 9.2 × 10^{-3} m^2/s),

*CORRESPONDING AUTHOR:
Shofia Karima, Master's Program in Earth Sciences, Faculty of Earth Sciences and Technology, Bandung Institute of Technology, Bandung 40132, Indonesia; Research Center for Geological Disaster, National Research and Innovation Agency, Bandung 40293, Indonesia; Email: shofia.karima@brin.go.id

ARTICLE INFO
Received: 26 February 2025 | Revised: 22 March 2025 | Accepted: 26 March 2025 | Published Online: 3 April 2025
DOI: https://doi.org/10.36956/eps.v4i1.2061

CITATION
Karima, S., Ningsih, N.S., Tisiana, A.R., et al., 2025. Water Mass Vertical Mixing in The Sulawesi Sea and Makassar Strait During the Second Transition Monsoon. Earth and Planetary Science. 4(1): 73–88. DOI: https://doi.org/10.36956/eps.v4i1.2061

followed by the homogeneous layer (K_z = 3.9 × 10^{-3} m^2/s), while the weakest is in the thermocline layer (K_z = 1.2 × 10^{-3} m^2/s). These patterns are influenced by the complex interaction of current dynamics and bathymetric features such as sills. The findings highlight the southern Makassar Strait (Transect 4) as a hotspot of vertical mixing and water mass transformation, playing a critical role in shaping ITF structure and the downstream transport of thermohaline properties.

Keywords: Richardson Number; Vertical Diffusivity; Sulawesi Sea; Vertical Mixing; Makassar Strait

1. Introduction

ITF brings Pacific Ocean water masses into Indonesian waters through two main routes. First, through the western route, enter the Sulawesi Sea and continue to the Makassar Strait, Flores Sea, and Banda Sea [1–3]. This pathway is known as the main transportation route of ITF [4,5]. The second pathway is the eastern pathway, through the Maluku Sea and Halmahera Sea, which then continues to the Banda Sea [6]. From the deep waters of the Indonesian oceans, this water mass flows into the Indian Ocean through major straits, such as the Lombok Strait and the strait between Alor and Timor [7].

The western pathway is the main pathway carrying about 11.6 ± 3.3 Sv (1 Sv = 10^6 m^3/s) of water mass from the North Pacific Ocean Subtropical thermocline (NPSW) and North Pacific Ocean Mid-layer (NPIW) [8,9]. A small portion of the water mass from the western pathway exits through the Lombok Strait at around 2.6 Sv [10,11], while most turn eastward into the Flores Sea, then into the Banda Sea, and finally exit through the Ombai Strait and Timor Gap [12].

Makassar Strait and Sulawesi Sea are important in flowing the ITF from the Pacific Ocean to the Indonesian Seas [13,14]. The water mass from the ITF contains the North Pacific and South Pacific water masses from Mindanao Current, as indicated by the availability of the maximum salinity value sourced from the subtropical area at the upper part of the thermocline [15–18]. After entering Indonesian waters, this salinity maximum weakens or even disappears due to vertical and lateral mixing with surrounding water masses, such as the low-salinity Bay of Bengal Water and waters from the Indonesian seas [16]. Based on Pranowo et al. [17], in the Makassar Strait, ranging from 13 m to 860 m depth, there are characteristics of seawater masses influenced by the type of Bengal Bay Water (BBW) that has salinity characteristics ranging from 28 $^0/_{00}$ to 35 $^0/_{00}$ [18].

Changes in water mass indicate the vertical mixing of seawater and turbulence, which is represented by vertical diffusivity (K_z) and Richardson number (R_i). Previous studies have obtained vertical diffusivity values for the Makassar Strait region's west, east, and transition I seasons. In the southeast monsoon season, the K_z value at Dewakang Sill is 2.84 × 10^{-4} m/s. In the same season, Gordon and Susanto state that the value of kinetic energy in shallower topography is more significant than in other locations [19]. The K_z value in the mixed layer depth has a value of 8.49 × 10^{-4} m^2/s; in the thermocline layer, K_z = 1 × 10^{-4} – 3.89 × 10^{-4} m^2/s and in the deep layer, it is 2.61 × 10^{-3} m^2/s [20].

In the Southeast season, the mixing value due to the influence of wind is greater than in the Northeast season, resulting in higher vertical mixing of water masses compared to other seasons [21]. The high intensity of wind stress also enhanced heat loss through heat flux. In addition, the Southeast Monsoon's current speed is greater in the northeast monsoon, according to current speed data from 2004 to 2009 [8]. Meanwhile, at the transition monsoon I, the value of K_z is 10^{-6}–10^{-2} m^2/s. Strong turbulent mixing at depths of 150 m and 300 m was identified, indicated by high values of K_z = 10^{-3}–10^{-2} m^2/s, which resulted in changes in the character of the ITF water mass [22]. The values of K_z Illustrate vertical mixing in the area. If the value is higher, the vertical mixing would be more intense than in other locations due to its unstable water column. Shear instability can be calculated as well by the Richardson number (R_i) to determine whether the turbulence occurred or was neglected.

Research related to water mass mixing that was specifically analyzed during the second transitional season has not been carried out. Thus, water mass mixing during the season will be analyzed using the Transport, Internal Waves, and Mixing in the Indonesian Throughflow Region (TIMIT) cruise data in October 2015. The results will be analyzed by the microscale vertical mixing characteristics using Thorpe's method. This method identifies turbulence overturns according to the water column stability. The Brunt Vaisala frequency is used to calculate the water column stability based on density data. In addition, the kinetic energy dissipation is required for the Thorpe method to identify the changes that occurred due to the instability [23,24].

2. Materials and Methods

Data used in this study were obtained from TIMIT Cruise 2015, conducted on October 1–18, 2015, a research project between the Ministry of Marine Affairs and Fisheries and the First Institute of Oceanography, China. The observation area consisted of 4 transects with 14 station points along the Makassar Strait to Lombok Strait, as shown in **Figure 1** and **Table 1.** This study divided the observed stations into four transects to facilitate analysis. The data used in this study are CTD (salinity, pressure, and temperature) and ADCP (current velocity) data.

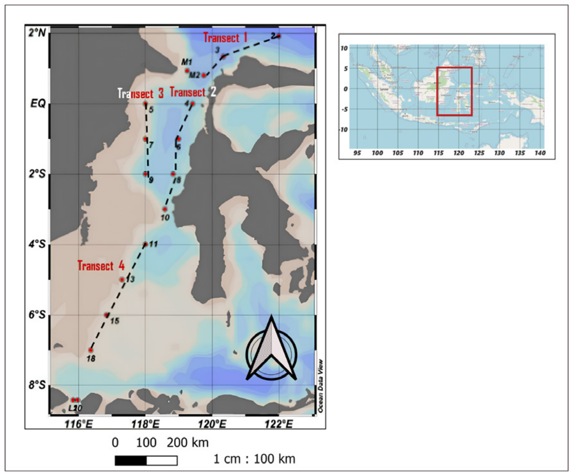

Figure 1. Location of Data Stations (Red Dots) and Transects (Black Dashed Lines).

Table 1. Characteristics of North Pacific Water Masses in the Sulawesi Sea and Makassar Strait (October 2015).

Transect 1				
No	**Type of Water Mass**	**Temperature (°C)**	**Salinity ($^{o}/_{oo}$)**	**Depth (m)**
1	Western North Pacific Subtropical Water	20	34.80	150
2	Pacific Equatorial Water	6–16	34.54–34.60	160–750
3	Western North Pacific Water	7–16	34.52–34.60	160–600
4	Northern Pacific Intermediate Water	7–11	34.42–34.57	350–560
Transect 2				
No	**Type of Water Mass**	**Temperature (°C)**	**Salinity ($^{o}/_{oo}$)**	**Depth (m)**
1	Western North Pacific Subtropical Water	20	34.80	130
2	Pacific Equatorial Water	6–16	34.54–34.60	160–750
3	Western North Pacific Water	7–16	34.52–34.60	160–580
4	Northern Pacific Intermediate Water	7–11	34.43–34.52	260–580
Transect 3				
No	**Type of Water Mass**	**Temperature (°C)**	**Salinity ($^{o}/_{oo}$)**	**Depth (m)**
1	Western North Pacific Subtropical Water	20	34.80	120
2	Pacific Equatorial Water	6–16	34.54–34.60	170–700
3	Western North Pacific Water	7–16	34.52–34.60	170–570
4	Northern Pacific Intermediate Water	7–11	34.41–34.52	260–570
Transect 4				
No	**Type of Water Mass**	**Temperature (°C)**	**Salinity ($^{o}/_{oo}$)**	**Depth (m)**
1	Western North Pacific Subtropical Water	-	-	-
2	Pacific Equatorial Water	6–16	34.54–34.60	137–580
3	Western North Pacific Water	7–16	34.51–34.60	137–745
4	Northern Pacific Intermediate Water	7–11	34.40–34.54	240–580

The initial step in studying vertical mixing involves determining the depths of the mixed, thermocline, and deep layers, as the analysis will be segmented into these three layers. The Brunt Väisälä frequency's value will indicate the water mass's stability. This is one of the parameters required to calculate kinetic energy dissipation and vertical diffusivity. Water mass transfer will also be analyzed using Thorpe displacement, the Thorpe scale, and the Ozmidov scale. The Ozmidov scale and Brunt Väisälä frequency will be calculated to obtain the vertical diffusivity (**Figure 2**).

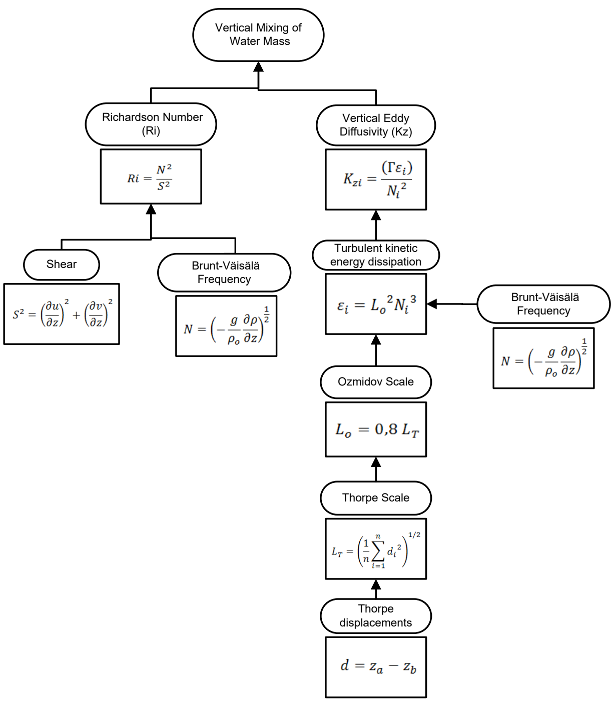

Figure 2. The Calculation of Vertical Mixing with the Richardson Number and Vertical Diffusivity.

The calculation of Brunt-Väisälä frequency squared (N^2) can be a determinant of the stability of a water column [25], which is calculated by the following equation:

$$N^2 = -\frac{g}{\rho_0}\frac{\partial\rho}{\partial z} \tag{1}$$

where N is the Brunt-Väisälä frequency (s^{-1}), g is gravity (m/s^2), ρ_0 is the reference density of seawater (kg/m^3), $\partial\rho$ is the density difference of the two depths (kg/m^3), ∂z is the depth difference (m). If the value of N^2 is positive, the water mass condition is stable. Meanwhile, if the value of N^2 is negative, the water mass does not oscillate, which means it is unstable. If the value of $N^2 = 0$, the water column is neutral.

Another parameter is the Richardson number, which shows the ratio of the stability of a stratified layer to the forces that destabilize it [1]. Mixing can occur if the Richardson value is between 0 and 0.25 ($0<R_i<0.25$) [26,27]. The equation used for the calculation of R_i is:

$$R_i = \frac{N^2}{\left(\frac{\partial u}{\partial z}\right)^2 + \left(\frac{\partial v}{\partial z}\right)^2} \tag{2}$$

where u is the zonal component of current (m/s), v is the meridional component of current (m/s), z is depth (m). The calculation of vertical diffusivity using the Thorpe method begins with the computation of the Thorpe scale. Before that, the Thorpe displacement (d, in m) must be determined. Thorpe displacement is the vertical distance a water parcel is moved from its observed, unstable position to a statically stable position [28], and is calculated as:

$$d = z_a - z_b \tag{3}$$

where z_a is the observed depth (m) and z_b is the depth after being in a stable condition (m).

In this study, we employed the Thorpe scale method to estimate turbulent overturns and associated mixing parameters. Thorpe scale (L_T, in m) is calculated as the root-mean-square displacement of all Thorpe displacements within the overturn:

$$L_T = \left(\frac{1}{n}\sum_{i=1}^{n} d_i^2\right)^{1/2} \tag{4}$$

where d_i represents the individual displacement of water parcels (m) and n is the amount of data. To determine the maximum turbulence scale constrained by stratification, the Thorpe scale was converted to the Ozmidov scale (L_0, in m) using the empirical relation [28]:

$$L_0 = 0.8L_T \tag{5}$$

The Ozmidov scale represents the largest vertical scale of turbulence that can be sustained in a stratified environment before being suppressed by buoyancy forces.

Subsequently, the rate of turbulent kinetic energy dissipation (ε, in W/kg), which quantifies the rate at which turbulent energy is lost due to viscous effects, using:

$$\varepsilon = L_0^2 N^3 \tag{6}$$

Once ε was obtained, the vertical eddy diffusivity (K_z, in m^2/s), which quantifies the effective mixing, was calculated using Osborn's formulation:

$$K_z = \frac{\Gamma \varepsilon}{N^2} \tag{7}$$

where Γ is the vertical mixing efficiency, taken as 0.2 following Osborn [29]. These steps provide methods for estimating vertical mixing from stratification and overturning data.

3. Results

3.1. Water mass characteristics in the Sulawesi Sea and Makassar Strait

ITF transports water masses from both the North Pacific and South Pacific Oceans. The western pathway of the ITF, which includes the Sulawesi Sea and Makassar Strait, is predominantly influenced by North Pacific water masses [30,31]. The temperature-salinity (T-S) diagrams in **Figure 3** illustrate the presence of characteristic North Pacific water masses along four observational transects in October 2015. Water mass identification follows the classification schemes of Guo et al. and Wyrtki [31,32], allowing for the identification of several characteristic North Pacific water masses: Western North Pacific Subtropical Water (WNPSW), Pacific Equatorial Water (PEW), Western North Pacific Water (WNPW), and North Pacific Intermediate Water (NPIW).

Across Transects 1 to 3, all four water masses were detected. However, at Transect 4, WNPSW was notably absent. This suggests that either substantial vertical mixing or transformation processes altered the water mass structure along the ITF pathway before reaching this southernmost transect.

The NPIW layer showed notable variation in salinity across the transects, which is further indicative of mixing processes. As summarized in **Table 1**, the NPIW had the highest salinity at Transect 1 (34.57 PSU) and the lowest at Transect 4 (34.40 PSU). These variations suggest progressive modification of the water masses as they transit southward, particularly through areas of rough topography such as the Dewakang Sill and the constricted Makassar Strait.

3.2. Water Column Stability in the Sulawesi Sea and Makassar Strait

In this study, the thermocline layer is identified using the method proposed by Yuliarinda et al. [33], which defines its upper and lower boundaries based on a minimum vertical temperature gradient of 0.1 °C/m (**Figure 4**). **Figure 4a** illustrates the vertical temperature profiles for each transect down to 1000 m. As expected, temperature consistently decreases with depth, with the thermocline boundaries marked by black lines [32].

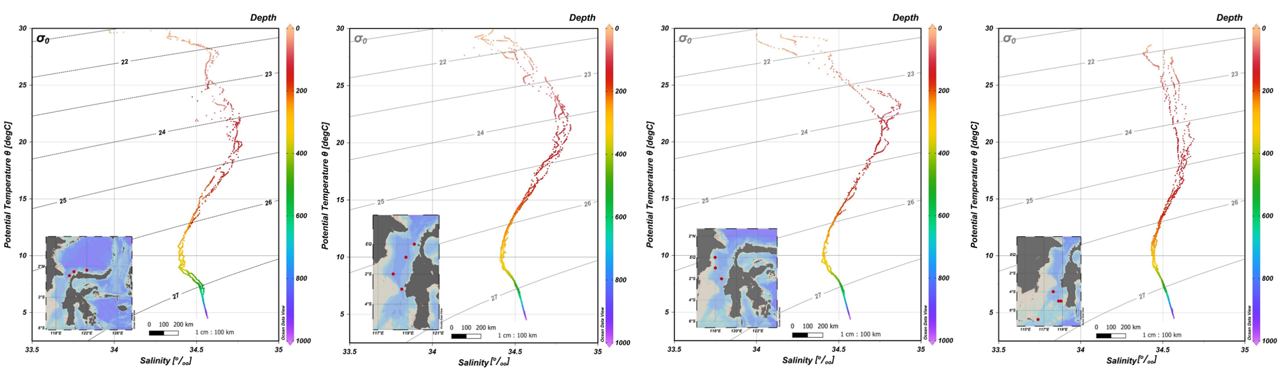

(a) (b) (c) (d)

Figure 3. Temperature - Salinity Diagrams Along Four Transects in the Sulawesi Sea and Makassar Strait in October 2015: **(a)** Transect 1, **(b)** Transect 2, **(c)** Transect 3, **(d)** Transect 4.

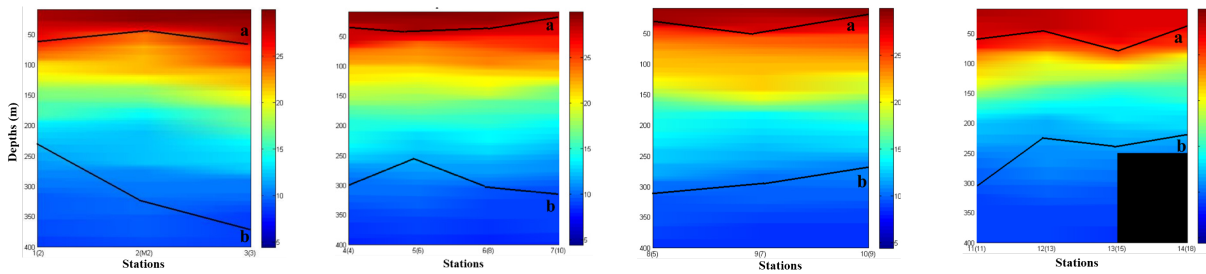

(a)

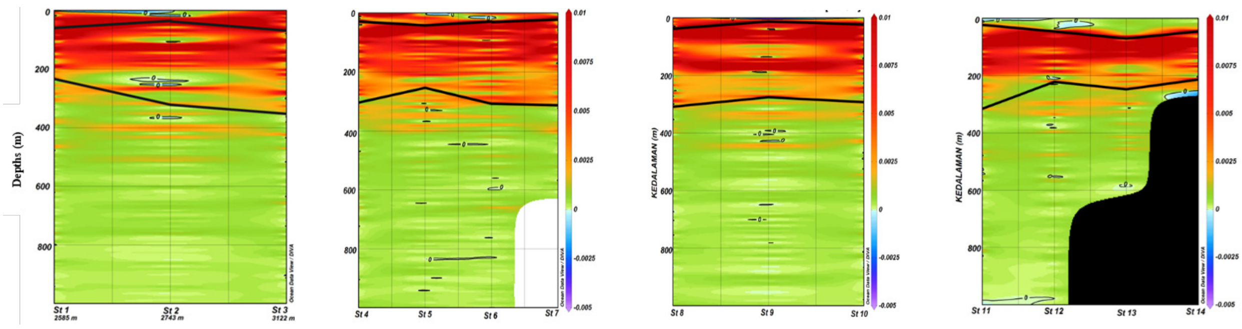

(b)

Figure 4. Vertical profiles of temperature and Brunt–Väisälä frequency (N^2) in the Sulawesi Sea and Makassar Strait (October 2015). **(a)** Vertical Temperature Profile (black lines). **(b)** Brunt–Väisälä Frequency (N^2) Profile for Depths of 0–400 m.

The stability of the water column was assessed using the Brunt–Väisälä frequency squared (N^2), as shown in **Figure 4b** for the upper 400 m of the water column. Positive N^2 values indicate stable stratification, which is observed in most transects. However, local instability is evident in specific regions. For instance, Station 14 exhibits a negative N^2 value (blue shading), which likely results from bathymetric disturbances (**Figure 5**). A similar instability is detected at Station 2 (**Figure 5a**), which is located near a shallow sill (**Figure 5b**), suggesting that bathymetric features contribute to local destabilization of the water column.

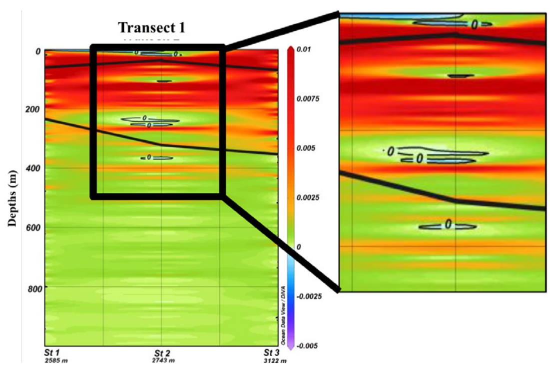

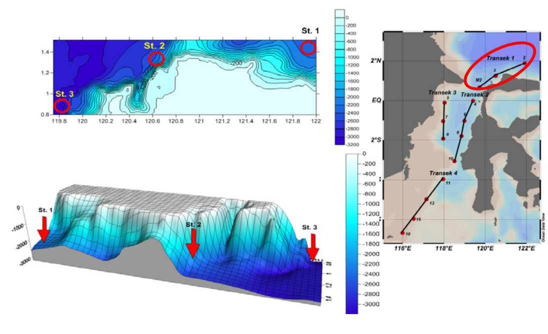

(a) (b)

Figure 5. Local water column instability and the influence of bathymetry. **(a)** Zoom out N^2 profile at Station 2; **(b)** Bathymetry profile (2D and 3D) at Transect 1.

The N^2 values vary substantially among the surface mixed layer, thermocline, and deeper layers, reflecting differences in vertical stratification and mixing potential. As shown in **Table 2**, the thermocline layer exhibits the highest average stability (7.0×10^{-3} s^{-2}), followed by the mixed layer (4.9×10^{-3} s^{-2}), while the deep layer is the least stable (0.6×10^{-3} s^{-2}).

The enhanced stability of the thermocline is attributed to the presence of the pycnocline—a density gradient that resists vertical motion. This layer also coincides with the core flow depth of the ITF (50–150 m), which has been reported to reach high velocities Shinoda et al. [34]. Gordon further supports this by identifying pronounced density differences within ITF layers that contribute to thermocline stability [35,36].

The lowest N^2 values were found in the deep layers across all transects, indicating reduced stability and a higher likelihood of vertical mixing. Transect 4 exhibited the lowest overall water column stability, likely due to its complex bathymetry, which ranges from 307 m to 1868 m in depth. This bathymetric variation can disrupt stratification and promote enhanced mixing processes.

Table 2. Average Brunt–Väisälä Frequency Squared (N^2) for Each Vertical Layer and Transect in October 2015.

Layer	Transect 1 (s^{-2})	Transect 2 (s^{-2})	Transect 3 (s^{-2})	Transect 4 (s^{-2})	Average per-layer (s^{-2})
Mixed Layer	5.7×10^{-3}	5.9×10^{-3}	5.5×10^{-3}	2.0×10^{-3}	4.9×10^{-3}
Thermocline Layer	7.8×10^{-3}	6.0×10^{-3}	6.7×10^{-3}	7.6×10^{-3}	7.0×10^{-3}
Deep Layer	0.3×10^{-3}	0.5×10^{-3}	0.5×10^{-3}	0.9×10^{-3}	0.6×10^{-3}
Average per-transect	4.6×10^{-3}	4.1×10^{-3}	4.2×10^{-3}	3.7×10^{-3}	4.2×10^{-3}

3.3. Quantification of Water Mass Mixing: Richardson Number Analysis

Vertical mixing in the water column was evaluated using the gradient Richardson number (R_i), which depends on both stratification (Brunt–Väisälä frequency, N^2) and vertical shear of horizontal currents. While Ri does not describe the mechanism of mixing, it serves as an indicator of turbulence occurrence [27,35]. **Figure 6** shows the current velocity profiles within the thermocline layer for multiple stations. Each station exhibits distinct velocity patterns. For example, Station 4 shows uniform flow direction with minor velocity variation, while Stations 3 and 7 exhibit upward-directed currents, contrasting with the generally downward flow observed at other stations [27,35].

The Ri values were computed and are visualized in **Figure 7**. Areas with $R_i > 0.25$ (white) indicates stable conditions where mixing is unlikely. In contrast, Ri values between 0 and 0.25 (ranging from purple to red) denote instability and potential turbulence [36]. Among all transects (**Figures 7a–d**), Transect 4 displays the deepest turbulent region, extending beyond 80 m, consistent with the vertical distribution of Ri values presented in **Table 3**.

The Richardson number is affected by the water stability and shear stress values. Turbulence is least likely to occur at Transect 1, with a frequency of approximately 56.14% (**Table 3**). The largest occurrence of turbulence is found at Transect 2 (73.33%), followed by Transect 3 and 4 (72.36%). The findings are consistent with Schiller's prior work, indicating that turbulence in the Makassar Strait exceeds that in the Sulawesi Sea [37–39].

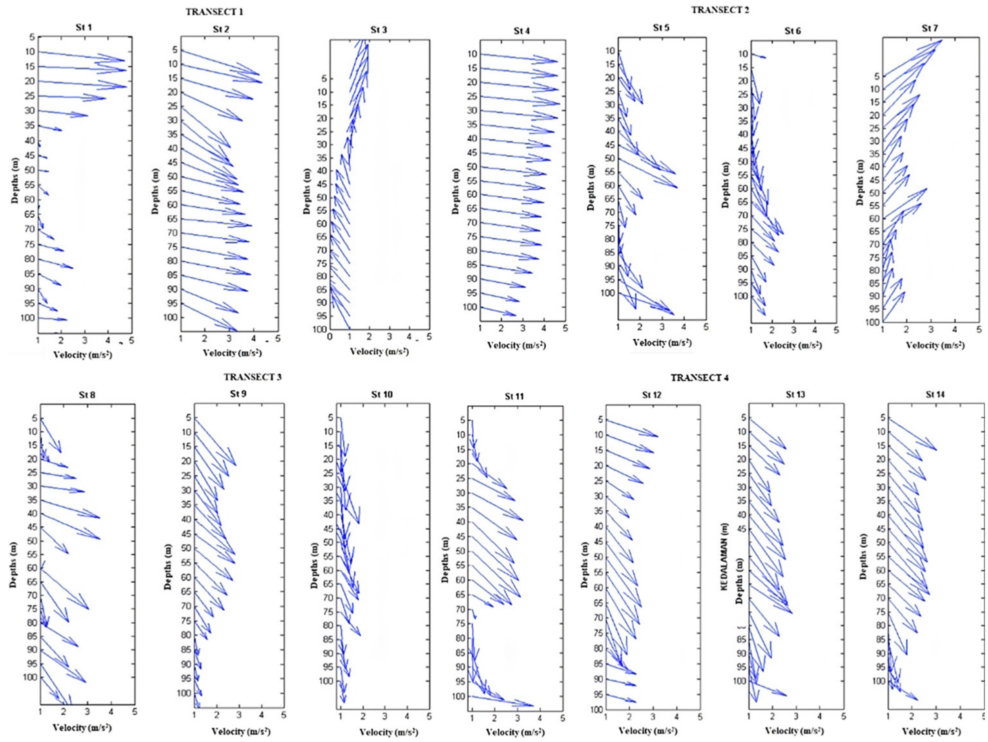

Figure 6. Current Velocity Profiles in the Sulawesi Sea and Makassar Strait in October 2015.

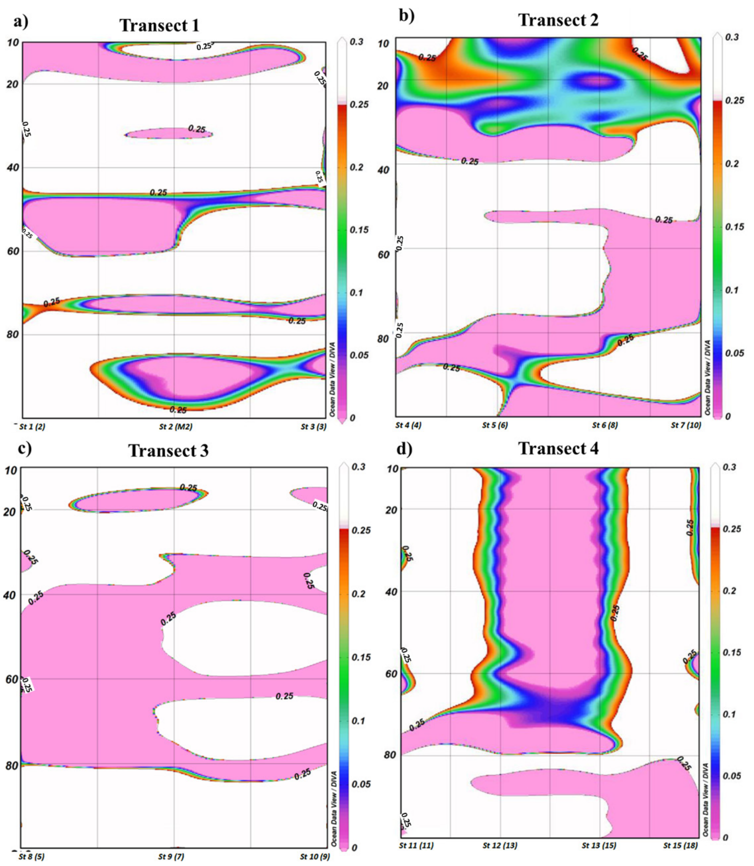

Figure 7. Richardson Number (R_i) Profiles Across Transects in October 2015. Color Gradients Indicate Mixing Likelihood: White (R_i > 0.25) = Stable; Red to Purple (R_i < 0.25) = Turbulent. **(a)** Transect 1, **(b)** Transect 2, **(c)** Transect 3, **(d)** Transect 4.

Table 3. Turbulence Frequency and Average Richardson Numbers (R_i) in the Sulawesi Sea and Makassar Strait (October 2015).

Transect	Turbulence (%)	R_i Number		
		Total	**≥ 0.25 (No turbulence)**	**≤ 0.25 (Turbulence)**
1	56.14	4.30	5.55	0.16
2	73.33	2.00	5.58	0.06
3	72.36	2.28	5.92	0.08
4	72.36	2.13	5.72	0.20
Average	68.54	2.68	5.69	0.12

3.4. Vertical Diffusivity from Thorpe Scale Analysis

Vertical diffusivity in this study was estimated using the Thorpe scale method, which quantifies vertical displacements of density anomalies as water parcels adjust from an unstable to a stable stratification (Thorpe displacements). **Figure 8** displays Thorpe displacement profiles across the Sulawesi Sea and Makassar Strait during the second transitional monsoon [40]. The displacements vary from near zero to more than 20 meters, with the highest values observed in Transect 4, particularly at Stations 2, 11, and 13 (**Figures 8a,b**).

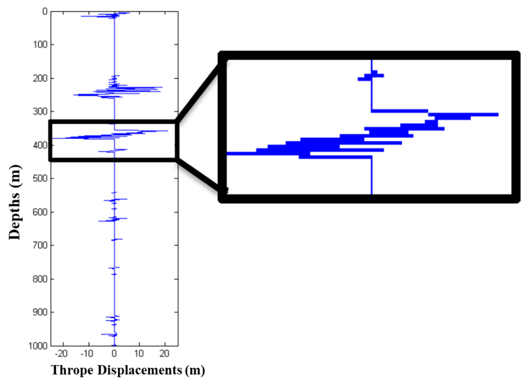

(a)

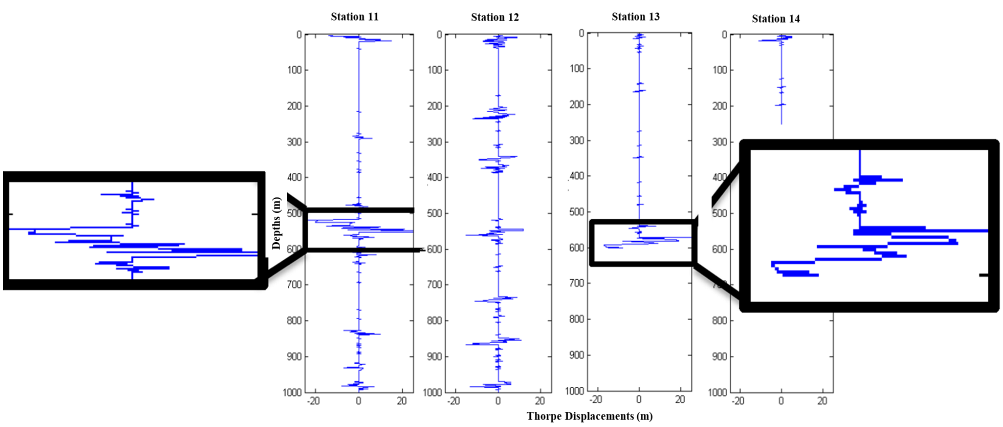

(b)

Figure 8. Zoom Out Results of the Thorpe Displacement Profile at **(a)** Station 2 (M2) and **(b)** Transect 4.

At Station 2, the pronounced displacements are likely influenced by its proximity to the Dewakang Sill, which generates strong internal wave activity. Similarly, bathymetric disturbances at Stations 11 and 13 amplify vertical instability. Across all stations, Thorpe displacements are generally low within the thermocline, reflecting the stable stratification that resists vertical motion [38,40].

The Thorpe scale in the mixed layer typically ranges from 0 to 0.8 m, while in deeper waters it increases substantially, reaching up to 4 m. This pattern corresponds with the Brunt-Väisälä frequency (N^2), which indicates reduced stratification at depth. Under such unstable conditions, the water column tends toward re-stratification, resulting in significant vertical displacements and elevated mixing.

Using the Thorpe scale, vertical diffusivity (K_z) was estimated from the dissipation rate of turbulent kinetic energy. **Figure 9** presents vertical profiles of K_z with the highest values consistently found in the deep layer of each transect (**Figures 9a–d**). Maximum diffusivity reached 9.2 × 10^{-3} m^2/s, coinciding with the lowest stability values (**Figure 4b**), suggesting enhanced mixing due to weakened stratification.

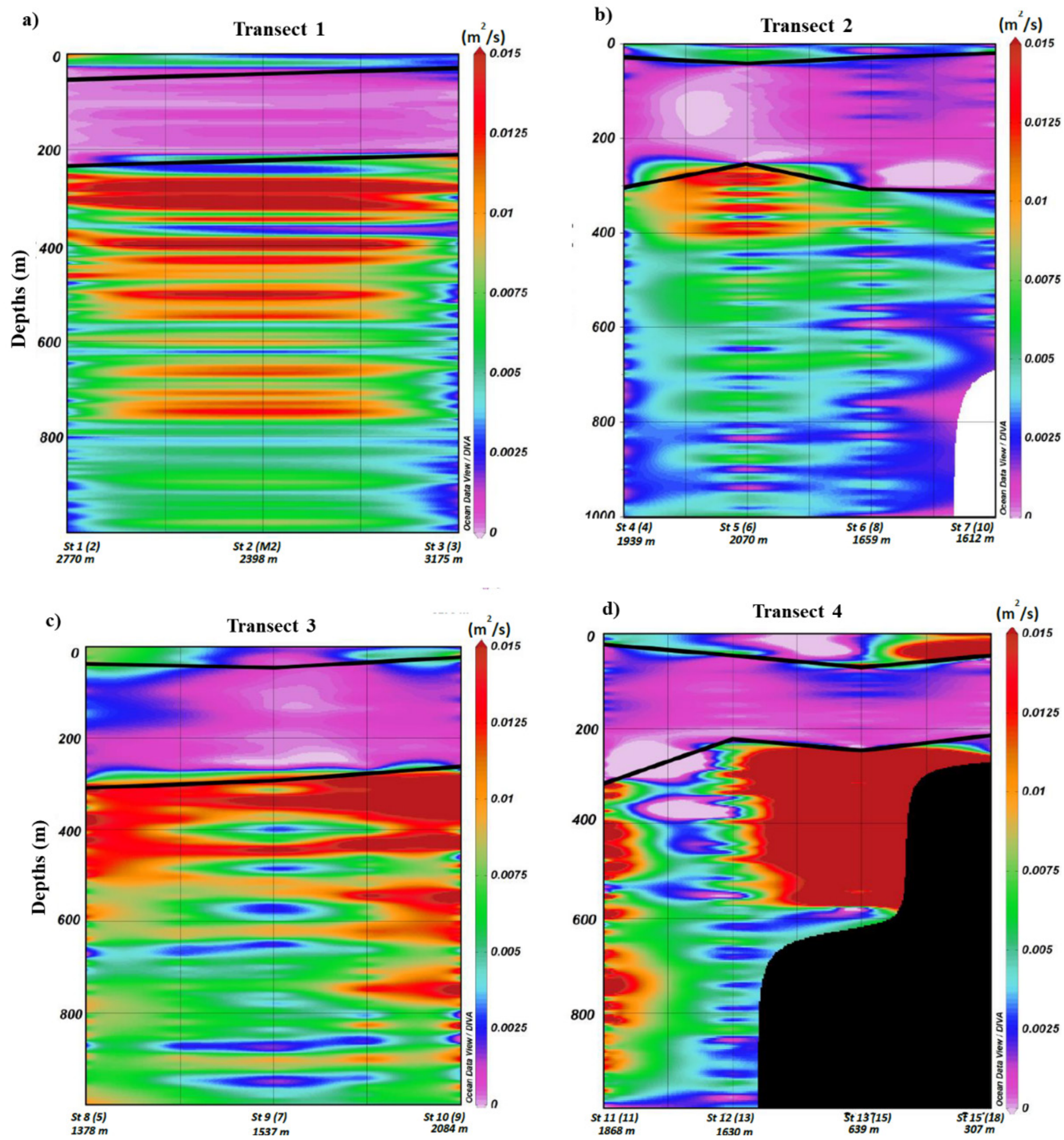

Figure 9. Vertical Diffusivity (K_z) Profiles in the Sulawesi Sea and Makassar Strait in October 2015. **(a)** Transect 1, **(b)** Transect 2, **(c)** Transect 3, and **(d)** Transect 4.

The homogenous layer is a layer that is affected by the atmospheric conditions above it. The K_z value in this layer is higher than the thermocline layer but lower than the deep layer. The extensive mixing in the homogenous layer is caused by the impact of the wind above it [25]. The thermocline layer has a low vertical diffusivity (K_z) of 1.2 × 10^{-3} m^2/s, resulting in minimal mixing compared to the inner layer. This is attributed to the presence of a pycnocline layer with a high stability value (**Table 3**), which would require considerable energy if turbulence occurred within this layer.

Each of the four transects has unique K_z values. The maximum K_z value is 8.5 × 10^{-3} m^2/s in Transect 4, and the lowest K_z value is 2.5 × 10^{-3} m^2/s in Transect 2. The varying bathymetric conditions in each region cause this. Transect 4 has shallow water depths of 625 m at Station 13 and 250 m at Station 14. Friction caused by the bathymetry might lead to intense vertical mixing at Transect 4. Transect 4 is located close to the Dewakang sill, which has the potential to induce internal waves. Internal waves have the potential to induce significant vertical mixing, as demonstrated by Hatayama [41].

Transect 1 has little bathymetric variability, resulting in less significant mixing than Transects 2 and 3, located in the Makassar Strait, or Transect 4, transitioning towards shallower waters entering the Java Sea. Transect 3 is located west of the Makassar Strait and has a lesser depth than Transect 2, so the bathymetry affects mixing in Transect 3. **Table 4** indicates that the K_z value is higher in Transect 3 compared to Transect 2.

In October 2015, the average K_z value in the Sulawesi Sea and Makassar Strait was 4.7 × 10^{-3} m^2/s. **Table 4** compares the calculated K_z values, which fall within the range reported in previous research. The parameters' values in this investigation are reported in **Table 5**.

Table 4. Vertical Diffusivity (K_z) by Layer and Transect (October 2015).

Layer	Transect 1 (m^2/s)	Transect 2 (m^2/s)	Transect 3 (m^2/s)	Transect 4 (m^2/s)	Average per Layer (m^2/s)
Mixed Layer	3.1 × 10^{-3}	2.9 × 10^{-3}	5.5 × 10^{-3}	3.9 × 10^{-3}	3.9 × 10^{-3}
Thermocline Layer	0.7 × 10^{-3}	0.7 × 10^{-3}	1.1 × 10^{-3}	2.8 × 10^{-3}	1.2 × 10^{-3}
Deep Layer	5.0 × 10^{-3}	4.0 × 10^{-3}	9.1 × 10^{-3}	18.0 × 10^{-3}	9.2 × 10^{-3}
Average per Transect	2.8 × 10^{-3}	2.5 × 10^{-3}	5.3 × 10^{-3}	8.5 × 10^{-3}	4.7 × 10^{-3}

Table 5. Summary of N^2, R_i, and K_Z Per Transect and Layer.

Transect	R_i	Shear stress ($\times 10^{-4}$ s^{-2})	N^2 ($\times 10^{-3}$ s^{-1})	K_z ($\times 10^{-3}$ s^{-1})	Layer	Depth (m)	N^2 ($\times 10^{-3}$ s^{-1})	K_z ($\times 10^{-3}$ s^{-1})
1	4.3	3.3	4.6	2.8	Mixed Layer	1–52	5.7	3.1
					Thermocline	53–310	7.8	0.7
					Deep Layer	311–1000	0.3	4.0
2	2.0	5.1	4.1	2.5	Mixed Layer	1–30	5.9	2.9
					Thermocline	31–295	6.0	0.7
					Deep Layer	296–1000	0.5	4.0
3	2.2	5.2	4.2	5.3	Mixed Layer	1–36	5.5	5.5
					Thermocline	37–288	6.7	1.1
					Deep Layer	289–1000	0.5	9.1
4	2.1	4.3	3.7	8.5	Mixed Layer	1–46	2.0	3.9
					Thermocline	47–250	7.6	2.8
					Deep Layer	251–1000	1.0	18.8

Ffield & Gordon reported a K_z value of around 10^{-4} in the thermocline layer [14]. This study found an average K_z value in the thermocline layer to be 12×10^{-4} m^2/s [14]. In the Labani Canal, the K_z value was measured at 2.4×10^{-4} m^2/s, but in the Dewakang Sill, the K_z value was higher at 2×10^{-1} m^2/s. The mean K_z value for all transects in the research was 4.7×10^{-3} m^2/s.

The mixing value is higher in the southeast season than in the northeast due to seasonal influences, such as stronger winds, measured explicitly at 2.84×10^{-4} m^2/s [21]. Based on the calculations in this study, transition season II has a higher vertical diffusivity value of 4.7×10^{-3} m^2/s. During the transition season, the most significant mixing occurred at depths of 150 m and 300 m, namely within the range of $K_z = 10^{-3}$–10^{-2} m^2/s. The study results indicate that the layers in each transect during transition season II had the highest mixing values, measuring 9.2×10^{-3} m^2/s.

The enhanced vertical diffusivity observed during the second transition monsoon (October 2015) is likely driven by a combination of seasonal wind forcing, weakened stratification, and the influence of topographic features such as sills and steep bathymetry. These conditions promote the generation of internal waves and shear instabilities, particularly in the deep layers and near constricted passages like the Dewakang Sill. The occurrence of maximum K_z values between 150 m and 300 m depths, within the lower thermocline and upper deep layers, indicate that this depth range is especially sensitive to energy inputs that drive mixing. This enhanced mixing during the transition season plays a critical role in vertical water mass exchange, nutrient fluxes, and thermohaline redistribution. The results suggest that the second transition monsoon contributes more significantly to vertical mixing than the northeast monsoon, which has weaker wind forcing. Therefore, the interplay between monsoonal dynamics and topographic controls is essential for understanding the spatiotemporal variability of mixing processes in semi-enclosed seas such as the Sulawesi Sea and Makassar Strait.

4. Discussion

The main focus of studying vertical mixing dynamics is ocean currents transported along the main ITF route. This includes the western route through the Sulawesi Sea, Makassar Strait, and Ombai Strait, as well as the eastern route through the Maluku Sea and Halmahera Sea [42,43]. The water mass originating from the Pacific Ocean introduces intricate conditions in Indonesian seas due to variations in salinity and thermocline features along its route. This research intends to investigate and comprehend the vertical mixing process using the vertical diffusivity value obtained using the Thorpe technique and the Richardson number [8,43]. The research aims to offer a more profound understanding of climate change, the dispersion of pollutants in the ocean, and global current dynamics, all essential for comprehending alterations in water masses and marine ecosystems.

The water moving from the Pacific Ocean to the Indian Ocean through the ITF route undergoes alterations in its properties in the deep waters of Indonesia [7]. ITF water mass salinity observations indicate variations at both the inlet and exit; it is also found in this study, where the maximum salinity is detected in Transect 1, and it is attenuated in Transect 4. The salinity of the NPSW water mass changed from 34.90 PSU to 34.54 PSU, while the salinity of the NPIW water mass changed from 34.35 PSU to 34.47 PSU [44–46]. The shift in salinity suggests a significant vertical mixing process occurring in the Indonesian seas [47]. This is supported by research indicating alterations in the water mass along the ITF route during transition season II, particularly the absence of the WNPSW water mass in Transect 4 (towards the Lombok Strait) [48–50]. Rough topography, like sills, straits, and internal wave action, can induce vertical mixing. Furthermore, variations in salinity have been found in every transect of the NPIW water mass, according to studies by Dwi Susanto et al. [51], Prihatiningsih et al. [50], and Susanto & Gordon [11].

The vertical mixing found in this study has the highest value in the Makassar Strait, with K_z value reaching up to 8.5×10^{-3} m^2/s. The number is higher than previous studies by Firdaus et al. and Hatayama et al. (2004) with the value of 5×10^{-3} m^2/s and 6×10^{-3} m^2/s, respectively [41,52]. It also significantly exceeds the average of K_z value in the Indonesian archipelago obtained from Ffield and Gordon (1992) and Koch Larrouy et al. at about 1×10^{-4} m^2/s to 1.5×10^{-4} m^2/s [14,53]. The results suggest enhanced mixing in Makassar Strait, likely due to strong throughflow from ITF, the complex bathymetry in the area, and internal wave activity in the region [54,55]. The K_z value obtained from this study will be beneficial for ocean modelling related to hydrodynamics, ecosystem, or sedimentation. It is also essential for studying climate change, oceanic contaminant dispersion, global current dynamics, and alteration in water mass composition [56,57].

5. Conclusions

This study demonstrated that vertical mixing is spatially and vertically heterogeneous in the ITF pathway. It is identified the existence of four primary water masses in the Sulawesi Sea and Makassar Strait during October 2015 is identified: Western North Pacific Subtropical Water (WNPSW), Pacific Equatorial Water (PEW), Western North Pacific Water (WNPW), and North Pacific Intermediate Water (NPIW). As water masses transit from the Sulawesi Sea to the Makassar Strait, particularly at depths of 120–150 m, WNPSW is no longer observed at the southernmost transect (Transect 4), indicating transformation through mixing processes. The Makassar Strait exhibited the highest levels of vertical mixing, as evidenced by low Richardson numbers (R_i = 2.0–2.2) and elevated vertical diffusivity values ($K_z = 8.5 \times 10^{-3}$ m^2/s). Turbulence occurred most frequently in this region, with 72.36–73.33% of the water column (within 10–100 m depth) experiencing mixing. In contrast, the Sulawesi Sea showed lower turbulence (56.14%) and a higher Ri value, indicative of more stable stratification. Vertical mixing varied by water column layer, with the thermocline exhibiting the lowest mixing intensity ($K_z = 1.2 \times 10^{-3}$ m^2/s), and the deep layer showing the highest ($K_z = 9.2 \times 10^{-3}$ m^2/s), consistent with observed stability profiles. Across the entire study area, the mean vertical diffusivity was 4.2×10^{-3} m^2/s, with the highest values concentrated in the southern Makassar Strait (Transect 4). Seasonal comparison reveals that mixing during the second transition monsoon ($K_z = 3.9 \times 10^{-3}$ to 4.7×10^{-3} m^2/s) is stronger than during the southeast monsoon and falls within the same range or exceeds the mixing intensity observed during the first transition season (from 10^{-3} to 10^{-2} m^2/s).

Future research suggested by this study is to explore the temporal variability of vertical mixing using long-term, high-resolution observations and modelling. The contribution of tidal and internal waves to mixing processes could provide deeper insight into the mixing mechanism in this area, specifically in the Labani Channel. In addition, the impact of water mass transformation would benefit regional climate and ecological studies.

Author Contributions

Conceptualization, S.K., N.S.N., A.R.T. and G.N.; methodology, S.K., N.S.N. and A.R.T.; software, S.K. and G.N.; validation, S.K., N.S.N. and A.R.T.; formal analysis, S.K., N.S.N., A.R.T. and G.N.; investigation, N.S.N. and A.R.T.; resources, A.R.T.; data curation, S.K. and A.R.T.; writing—original draft preparation, G.N. and S.K.; writing—review and editing, N.S.N. and A.R.T.; visualization, G.N. and S.K.; supervision, N.S.N. and A.R.T.; funding acquisition, A.R.T. All authors have read and agreed to the published version of the manuscript.

Funding

This research received no external funding.

Institutional Review Board Statement

Not applicable.

Informed Consent Statement

Not applicable.

Data Availability Statement

Data are available from the corresponding author upon reasonable request.

Acknowledgments

The authors would like to thank the anonymous reviewers for their valuable comments and suggestions that helped improve the quality of this manuscript.

Conflicts of Interest

The authors declare no conflict of interest.

References

[1] Panjaitan, F.A.P., Wulandari, S.Y., Handoyo, G., et al., 2021. Identification and Stratification of Water Masses in the Sulawesi Sea [in Indonesian]. Indonesian Journal of Oceanography. 3(3), 322–331. DOI: https://doi.org/10.14710/IJOCE.V3I3.12255

[2] Yudowaty, S.O., Radjawane, I.M., Fajary, R., et al., 2025. Heat Transport Variability Within the Inlet and Outlet of Makassar Strait. Malaysian Applied Geography. 3(1), 38–44.

[3] Napitupulu, G., Fekranie, N.A., Millina, A.V., et al., 2025. Seasonal Variability of Surface Heat Transport in the Banda Sea. Thalassas: An International Journal of Marine Sciences. 41(2), 1–20. DOI: https://doi.org/10.1007/S41208-025-00840-4

[4] Yuliardi, A.Y., Prayogo, L.M., Joesidawati, M.I., et al., 2022. Dynamics of the Spatial-Vertical Distribution of Water Masses in the West and East Indonesian Throughflow Routes in the Wet Season [in Indonesian]. Jurnal Miyang: Ronggolawe Fisheries and Marine Science Journal. 2(2), 38–46. DOI: https://doi.org/10.55719/JMIY.V2I2.532

[5] Ilahude, A.G., Gordon, A.L., 1996. Thermocline stratification within the Indonesian Seas. Journal of Geophysical Research: Oceans. 101(C5), 12401–12409.

[6] Wang, S., Ummenhofer, C.C., Oppo, D.W., et al., 2023. Freshwater Contributions to Decadal Variability of the Indonesian Throughflow. Geophysical Research Letters. 50(14), e2023GL103906. DOI: https://doi.org/10.1029/2023GL103906

[7] Fieux, M., Molcard, R., Ilahude, A.G., 1996. Geostrophic transport of the Pacific-Indian Oceans throughflow. Journal of Geophysical Research: Oceans. 101(C5), 12421–12432. DOI: https://doi.org/10.1029/95JC03566

[8] Gordon, A.L., Susanto, R.D., Ffield, A., et al., 2008. Makassar Strait throughflow, 2004 to 2006. Geophysical Research Letters. 35(24). DOI: https://doi.org/10.1029/2008GL036372

[9] Rugebregt, M.J., Hudiyono, S., Utomo, S.W., et al., 2023. Indonesian Through-Flow Water Mass Circulation in the Makassar Strait and Lombok Strait, Indonesia. Migration Letters. 20(S2), 1190–1198.

[10] Sprintall, J., Wijffels, S.E., Molcard, R., et al., 2009. Direct estimates of the Indonesian Throughflow entering the Indian Ocean: 2004–2006. Journal of Geophysical Research: Oceans. 114(C7), 7001. DOI: https://doi.org/10.1029/2008JC005257

[11] Susanto, R.D., Gordon, A.L., 2005. Velocity and transport of the Makassar Strait throughflow. Journal of Geophysical Research: Oceans. 110(C1), 1–10. DOI: https://doi.org/10.1029/2004JC002425

[12] Guo, Y., Li, Y., Yang, D., et al., 2023. Water sources of the Lombok, Ombai and Timor outflows of the Indonesian throughflow. Frontiers in Marine Science. 10, 1326048. DOI: https://doi.org/10.3389/fmars.2023.1326048

[13] Atmadipoera, A., Molcard, R., Madec, G., et al., 2009. Characteristics and variability of the Indonesian throughflow water at the outflow straits. Deep Sea Research Part I: Oceanographic Research Papers. 56(11), 1942–1954. DOI: https://doi.org/10.1016/J.DSR.2009.06.004

[14] Ffield, A., Gordon, A.L., 1992. Vertical Mixing in the Indonesian Thermocline. Journal of Physical Oceanography. 22(2), 184–195.

[15] Larasati, O.D.D., Hendrizan, M., Rachmayani, R., et al., 2024. VARIABILITY OF SEA SURFACE TEMPERATURE AND SALINITY IN MAKASSAR STRAIT DURING THE LAST GLACIAL MAXIMUM. BULLETIN OF THE MARINE GEOLOGY. 39(2). DOI: https://doi.org/10.32693/BOMG.39.2.2024.882

[16] Murray, S.P., Arief, D., 1988. Throughflow into the Indian Ocean through the Lombok Strait, January 1985–January 1986. Nature. 333(6172), 444–447. DOI: https://doi.org/10.1038/333444a0

[17] Gordon, A.L., 1986. Interocean exchange of thermocline water. Journal of Geophysical Research: Oceans. 91(C4), 5037–5046. DOI: https://doi.org/10.1029/JC091IC04P05037

[18] setiyo Pranowo, W., Nurhidayat, N., Asmoro, N.W., 2022. Characteristic of Temperature and Salinity in The Makassar Strait Based on Arlindo 2005 and Timit 2015 CTD Cruise Data [in Indonesian]. Jurnal Chart Datum. 8(2), 107–116. DOI: https://doi.org/10.37875/CHARTDATUM.V8I2.144

[19] Gordon, A.L., Susanto, R.D., 1998. Makassar Strait transport: Initial estimate based on Arlindo results. Marine Technology Society Journal. 32(4), 34.

[20] Anshari, A.I., 2023. Identification of Surface Current Patterns in Small Pelagic Fishing Areas in the Western Season of the Spermonde Islands, Indonesia. Asian Journal of Advanced Research and Reports. 17(8), 80–87. DOI: https://doi.org/10.9734/AJARR/2023/V17I8506

[21] Atmadipoera, A.S., Jaya, I., Sudjono, E.H., 2017. Analysis of turbulent mixing in Dewakang Sill, Southern Makassar Strait. IOP Conference Series: Earth and Environmental Science. 54(1),

012086. DOI: https://doi.org/10.1088/1755-1315/54/1/012086

[22] Atmadipoera, A.S., Widyastuti, P., 2014. A NUMERICAL MODELING STUDY ON UPWELLING MECHANISM IN SOUTHERN MAKASSAR STRAIT. Jurnal Ilmu dan Teknologi Kelautan Tropis. 6(2), 355–371. DOI: https://doi.org/10.29244/JITKT.V6I2.9012

[23] Naulita, Y., 2016. TURBULENT MIXING PROCESSES IN LABANI CHANNEL, THE MAKASSAR STRAIT. Jurnal Ilmu dan Teknologi Kelautan Tropis. 8(1), 345–355.

[24] Finnigan, T.D., Luther, D.S., Lukas, R., 2002. Observations of Enhanced Diapycnal Mixing near the Hawaiian Ridge. Journal of Physical Oceanography. 32(11), 2988–3002. DOI: https://doi.org/10.1175/1520-0485(2002)032<2988:OOEDMN>2.0.CO;2

[25] Purwandana, A., Purba, M., Atmadipoera, A.S., 2014. Distribution of Turbulence Mixing in Alor Strait [in Indonesian]. Ilmu Kelautan. 19(1), 43–54. DOI: https://doi.org/10.14710/IK.IJMS.19.1.43-54

[26] Pond, S., Pickard, G.L., 1983. Introductory dynamical oceanography. Gulf Professional Publishing: Houston, TX, USA. pp. 1–329.

[27] Richardson, M.L.F., 1920. The supply of energy from and to atmospheric eddies. Proceedings of the Royal Society of London. Series A, Containing Papers of a Mathematical and Physical Character. 97(686), 354–373. DOI: https://doi.org/10.1098/RSPA.1920.0039

[28] Purwandana, A., 2013. Study of Vertical Water Mass Mixing and Its Benefits [in Indonesian]. Jurnal Oseana. 38(3), 9–22.

[29] Dillon, T.M., 1982. Vertical overturns: A comparison of Thorpe and Ozmidov length scales. Journal of Geophysical Research: Oceans. 87(C12), 9601–9613. DOI: https://doi.org/10.1029/JC087IC12P09601

[30] Wang, Z., Yin, X., Li, X., et al., 2023. Water Mass Variations in the Maluku Channel of the Indonesian Seas During the Winter of 2018–2019. Journal of Geophysical Research: Oceans. 128(3), e2022JC018731. DOI: https://doi.org/10.1029/2022JC018731

[31] Wyrtki, K., 1961. The thermohaline circulation in relation to the general circulation in the oceans. Deep Sea Research. 8(1), 39–64. DOI: https://doi.org/10.1016/0146-6313(61)90014-4

[32] Guo, X.Y., Zhu, X.H., Long, Y., et al., 2013. Spatial variations in the Kuroshio nutrient transport from the East China Sea to south of Japan. Biogeosciences. 10(10), 6403–6417. DOI: https://doi.org/10.5194/BG-10-6403-2013

[33] Yuliarinda, R.E., Muslim, M., Atmodjo, W., 2013. Studi Struktur Lapisan Termoklin di Perairan Selat Makassar [in Indonesian]. Jurnal Oceanografi. 1(1), 33–39.

[34] Shinoda, T., Han, W., Metzger, E.J., et al., 2012. Seasonal Variation of the Indonesian Throughflow in Makassar Strait. Journal of Physical Oceanography. 42(7), 1099–1123. DOI: https://doi.org/10.1175/JPO-D-11-0120.1

[35] Gordon, A.L., 2005. The indonesian seas. Oceanography. 18(4), 14.

[36] Delpeche, N.C., Soomere, T., Lilover, M.-J., 2010. Diapycnal mixing and internal waves in the Saint John River Estuary, New Brunswick, Canada with a discussion relative to the Baltic Sea. Estonian Journal of Engineering. 16(2), 157–175. DOI: https://doi.org/10.3176/eng.2010.2.05

[37] Utama, F.G., Atmadipoera, A.S., Purba, M., et al., 2017. Analysis of upwelling event in Southern Makassar Strait. IOP Conference Series: Earth and Environmental Science. 54(1), 012085. DOI: https://doi.org/10.1088/1755-1315/54/1/012085

[38] Napitupulu, G., Fekranie, N.A., Nurdjaman, S., et al., 2023. Analysis of Upwelling Variations Caused by ENSO Intensification in the Southern Makassar Strait. Proceedings of the International Conference on Radioscience, Equatorial Atmospheric Science and Environment and Humanosphere Science (INCREASE 2022); 22–23 November 2022; Indonesia (online). pp. 437–448. DOI: https://doi.org/10.1007/978-981-19-9768-6_41

[39] Napitupulu, G., Nurdjaman, S., Fekranie, N.A., et al., 2022. Analysis of Upwelling in the Southern Makassar Strait in 2015 Using Aqua-Modis Satellite Image. Journal of Water Resources and Ocean Science. 11(4), 64–70.

[40] Schiller, A., 2004. Effects of explicit tidal forcing in an OGCM on the water-mass structure and circulation in the Indonesian throughflow region. Ocean Modelling. 6(1), 31–49. DOI: https://doi.org/10.1016/S1463-5003(02)00057-4

[41] Hatayama, T., 2004. Transformation of the Indonesian throughflow water by vertical mixing and its relation to tidally generated internal waves. Journal of Oceanography. 60(3), 569–585. DOI: https://doi.org/10.1023/B:JOCE.0000038350.32155.CB

[42] McCreary, J.P., Miyama, T., Furue, R., et al., 2007. Interactions between the Indonesian Throughflow and circulations in the Indian and Pacific Oceans. Progress in Oceanography. 75(1), 70–114. DOI: https://doi.org/10.1016/J.POCEAN.2007.05.004

[43] Wajsowicz, R.C., Gordon, A.L., Ffield, A., et al., 2003. Estimating transport in Makassar Strait. Deep Sea Research Part II: Topical Studies in Oceanography. 50(12–13), 2163–2181. DOI: https://doi.org/10.1016/S0967-0645(03)00051-1

[44] Gordon, A.L., Susanto, R.D., Ffield, A., 1999. Throughflow within Makassar Strait. Geophysical Research Letters. 26(21), 3325–3328. DOI: https://doi.org/10.1029/1999GL002340

[45] Susanto, R.D., Gordon, A.L., Sprintall, J., et al., 2000. Intraseasonal variability and tides in Makassar Strait. Geophysical Research Letters. 27(10), 1499–1502. DOI: https://doi.org/10.1029/2000GL011414

[46] Gordon, A.L., Napitu, A., Huber, B.A., et al., 2019. Makassar Strait Throughflow Seasonal and Interannual Variability: An Overview. Journal of Geophysical Research: Oceans. 124(6), 3724–3736. DOI: https://doi.org/10.1029/2018JC014502

[47] Susanto, R.D., Wei, Z., Adi, R.T., et al., 2013. Observations of the Karimata Strait througflow from December 2007 to November 2008. Acta Oceanologica Sinica. 32(5), 1–6. DOI: https://doi.org/10.1007/S13131-013-0307-3

[48] Susanto, R.D., Gordon, A.L., Sprintall, J., 2007. Observations and proxies of the surface layer throughflow in Lombok Strait. Journal of Geophysical Research: Oceans. 112(C3), 1–6. DOI: https://doi.org/10.1029/2006JC003790

[49] Susanto, R.D., Ray, R.D., 2022. Seasonal and Interannual Variability of Tidal Mixing Signatures in Indonesian Seas from High-Resolution Sea Surface Temperature. Remote Sensing. 14(8), 1934. DOI: https://doi.org/10.3390/RS14081934

[50] Prihatiningsih, I., Jaya, I., Atmadipoera, A.S., et al., 2019. Turbulent mixing of water masses in Selayar Slope - Southern Makassar Strait. IOP Conference Series: Earth and Environmental Science. 284(1), 012033. DOI: https://doi.org/10.1088/1755-1315/284/1/012033

[51] Susanto, R.D., Ffield, A., Gordon, A.L., et al., 2012. Variability of Indonesian throughflow within Makassar Strait, 2004–2009. Journal of Geophysical Research: Oceans. 117(C9), 9013. DOI: https://doi.org/10.1029/2012JC008096

[52] Firdaus, M., Rahmawitri, H., Haryoadji, S., et al., 2021. Indirect estimation of turbulent mixing in western route of Indonesian throughflow. IOP Conference Series: Earth and Environmental Science. 944(1), 012059. DOI: https://doi.org/10.1088/1755-1315/944/1/012059

[53] Koch-Larrouy, A., Madec, G., Bouruet-Aubertot, P., et al., 2007. On the transformation of Pacific Water into Indonesian Throughflow Water by internal tidal mixing. Geophysical Research Letters. 34(4). DOI: https://doi.org/10.1029/2006GL028405

[54] Tillinger, D., Gordon, A.L., 2010. Transport weighted temperature and internal energy transport of the Indonesian throughflow. Dynamics of Atmospheres and Oceans. 50(2), 224–232. DOI: https://doi.org/10.1016/j.dynatmoce.2010.01.002

[55] Osborn, T.R., 1980. Estimates of the Local Rate of Vertical Diffusion from Dissipation Measurements. Journal of Physical Oceanography. 10(1), 83–89. DOI: https://doi.org/10.1175/1520-0485(1980)010<0083:EOTLRO>2.0.CO;2

[56] Gordon, A.L., Sprintall, J., Van Aken, H.M., et al., 2010. The Indonesian throughflow during 2004–2006 as observed by the INSTANT program. Dynamics of Atmospheres and Oceans. 50(2), 115–128. DOI: https://doi.org/10.1016/J.DYNATMOCE.2009.12.002

[57] Gordon, A.L., Huber, B.A., Metzger, E.J., et al., 2012. South China Sea throughflow impact on the Indonesian throughflow. Geophysical Research Letters. 39(11). DOI: https://doi.org/10.1029/2012GL052021